Molecular Cell, Vol. 3, 761–770, June, 1999, Copyright ©1999 by Cell Press

Functional Organization of Clathrin in Coats: Combining Electron Cryomicroscopy and X-Ray Crystallography

Andrea Musacchio,[1,6,7] Corinne J. Smith,[4,6] Alan M. Roseman,[4] Stephen C. Harrison,[1,2] Tomas Kirchhausen,[3,5] and Barbara M. F. Pearse[4]
[1]Children's Hospital
[2]Howard Hughes Medical Institute
Laboratory of Molecular Medicine
[3]Department of Cell Biology and
Center for Blood Research
Harvard Medical School
Boston, Massachusetts 02115
[4]Medical Research Council Laboratory
of Molecular Biology
Hills Road
Cambridge CB2 2QH
United Kingdom

Summary

The sorting of specific proteins into clathrin-coated pits and the mechanics of membrane invagination are determined by assembly of the clathrin lattice. Recent structures of a six-fold barrel clathrin coat at 21 Å resolution by electron cryomicroscopy and of the clathrin terminal domain and linker at 2.6 Å by X-ray crystallography together show how domains of clathrin interact and orient within the coat and reveal the strongly puckered shape and conformational variability of individual triskelions. The β propeller of the terminal domain faces the membrane so that recognition segments from adaptor proteins can extend along its lateral grooves. Clathrin legs adapt to different coat environments in the barrel by flexing along a segment at the knee that is free of contacts with other molecules.

Introduction

Clathrin organizes membrane vesiculation from the cell surface and from some internal compartments, by forming coats together with adaptors, receptors, and other membrane-associated proteins (for reviews see Pearse and Robinson, 1990; Kirchhausen et al., 1997; Robinson, 1997; Schmid, 1997). Electron micrographs of sectioned cells capture images of coated pits and vesicles at various stages of budding into the cytoplasm (Perry and Gilbert, 1979), and rapid freeze, deep etch pictures of the cytoplasmic surface of fibroblasts reveal flat, hexagonal lattices as well as deeply invaginated buds with a mixture of hexagons and pentagons (Heuser, 1980).

The regulation of clathrin assembly and uncoating and the selection of membrane proteins for inclusion in coated pits and vesicles require participation of adaptor complexes (reviewed in Kirchhausen et al., 1997; Schmid, 1997). AP-1 adaptor complexes function primarily at the *trans*-Golgi network, and the related AP-2 adaptors occur in plasma membrane–coated pits (Robinson, 1987; Ahle et al., 1988). AP-2s link endocytic receptors (for example, transferrin and EGF receptors) to the clathrin coat and interact with components such as Eps15, amphyphysin, and dynamin thought to be needed for vesicle formation and closure (Kirchhausen et al., 1997; Wigge et al., 1997; Benmerah et al., 1998; Chen et al., 1998; Cupers et al., 1998). There also appear to be more specialized adaptors (for example, the non-visual arrestins) that bridge between G-coupled receptors and clathrin (Goodman et al., 1997).

Purified clathrin coats exhibit a range of structures (Crowther et al., 1976). Any closed-shell lattice based on a hexagonal net must have 12 pentagons, and one common design is the six-fold barrel, with hexagons at either pole, each surrounded by six pentagons, and with six hexagons around the equator (Figure 1A). The unusual triskelion shape of the clathrin trimer (Figure 1B), first revealed in rotary shadowed preparations (Ungewickell and Branton, 1981), leads to a remarkably extended set of interactions within such a lattice (Crowther and Pearse, 1981). A triskelion contains three identical, 190 kDa heavy chains and three, approximately 30 kDa, light chains, of which there are several related forms (Kirchhausen and Harrison, 1981; Ungewickell and Branton, 1981; Jackson et al., 1987; Kirchhausen et al., 1987a, 1987b).

Reconstitution of "cages" from purified clathrin and of "coats" from clathrin plus adaptors under conditions favoring formation of hexagonal barrels (Pearse and Robinson, 1984) provided specimens for study by electron cryomicroscopy. Reconstructions of tilted images showed that coats have three shells of density corresponding respectively to the outer clathrin lattice, the heavy chain N-terminal domains, and an inner layer of adaptors (Vigers et al., 1986a, 1986b). Recently, a much improved reconstruction of a clathrin/AP-2 coat, at 21 Å resolution, has revealed details of how the proximal and distal legs form the polyhedral cage (Smith et al., 1998). It also shows the terminal domains as hook-like features linking the surface of the layer of adaptor complexes with the lattice of the barrel.

Strategies for studying clathrin by X-ray crystallography have involved attempts to assemble uniform small cages (Sorger et al., 1986) as well as efforts to dissect the molecule into domains (Kirchhausen and Harrison, 1984). The sequence of the 1675 amino acid residues in a clathrin heavy chain, derived from the sequence of its cDNA, permitted mapping of defined cleavage points onto the contour of a triskelion leg (Kirchhausen et al., 1987a). The globular N-terminal domain at the tip and a segment linking it to the distal leg together comprise residues 1–500 (approximately), and the three-fold vertex contains the heavy chain C terminus. The crystal structure of a recombinant terminal domain–linker fragment, reported recently, shows that the terminal domain is a seven-blade β propeller, similar to those formed by WD repeats (Ter Haar et al., 1998). Its grooved perimeter is likely to present interaction sites for various adaptor

[5]To whom correspondence should be addressed (e-mail:kirchhausen@crystal.harvard.edu).
[6]These authors contributed equally to this work.
[7]Present address: Department of Experimental Oncology, European Institute of Oncology, via Ripamonti 435, 20141 Milan, Italy.

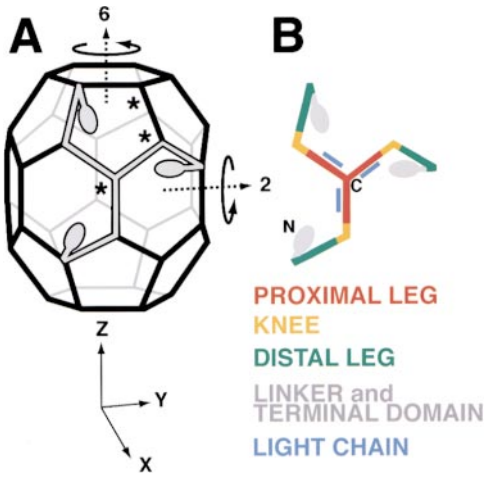

Figure 1. A Clathrin Triskelion and Its Position in a Barrel Coat

(A) Diagram of the lattice of a clathrin barrel with one triskelion in place. The barrel is oriented approximately with one of its two-fold axes in the direction of the viewer, and it is slightly rotated about another two-fold axis parallel to the page, to show the six-fold axis running through the polar hexagonal faces. The stars show examples of the three symmetry-distinct vertices in this structure.

(B) Schematic representation of a clathrin triskelion, showing orientations of the heavy and light chains and the principal heavy chain segments. The color scheme introduced here is used throughout this paper. Proximal legs are in red, knees in yellow, distal legs in green, and linker and terminal domain in gray.

proteins. The linker is a zigzag of α helical segments, which stack to form a stiff, but not utterly rigid, rod. We proposed that this α zigzag extends along most or all of the triskelion leg, and the structure of a segment from the proximal leg, recently crystallized (Ybe et al., 1998), may soon clarify this point.

We have now used the 2.6 Å resolution crystal structure of the terminal domain and linker and an approximate molecular analysis of the 21 Å electron cryomicroscopy (cryoEM) reconstruction to study the orientation of the terminal domain within a coat and to analyze clathrin packing in more detail. As described previously, a leg spans two edges of a polygon and ends in the hook-like feature identified as the terminal domain (Smith et al., 1998). The crystallographically determined model of the terminal domain–linker gives a good fit to this density. The "top" surface of the propeller faces the adaptor cluster that lies within the clathrin lattice. Moreover, by constructing a triskelion representation that can be rotated and compared, we have been able to determine how a leg flexes at various positions in the barrel. In this commonly found structure, all three symmetry-distinct triskelions have identical puckers at their vertices, and most of the conformational variability is restricted to the "knee." We discuss the implications of these findings for control of clathrin assembly and for the formation of larger coats and flat arrays.

Results

Orientation of Terminal Domains within a Coat

The crystal structure of a 55 kDa clathrin heavy chain fragment includes the globular N-terminal domain and as well as part of the linker region (Ter Haar et al., 1998). The conformations and relative orientations of the β propeller terminal domain and the α zigzag linker impart an overall hook-like shape to the fragment. Since the evidence that the hook-like features seen in the electron microscopy (EM) map (Smith et al., 1998) correspond to clathrin terminal domains is compelling, we extracted these features from the EM map and positioned the X-ray structure within them using a density correlation procedure described in Experimental Procedures. The resulting positions for each terminal domain on a pentagonal face are displayed in Figure 2. The fit varies slightly among the nine independent domains, probably because of intrinsic noise in the EM map, conformational variability of the domains within a cage, constraints imposed by adaptor complexes, and variability among individual particles in the preparation. A higher resolution EM map is likely to help distinguish among these factors.

Modeling Clathrin in the Image Reconstruction from Electron Cryomicroscopy

Electron microscopy of free clathrin shows that the legs are relatively uniform rods (Kirchhausen and Harrison, 1981, 1984; Ungewickell and Branton, 1981). The 21 Å cryoEM reconstruction has sufficient clarity that one can follow the individual rod-like legs as they radiate from the three-fold vertex of a triskelion, and a general description of the course of a leg has been provided in the paper on the reconstruction (Smith et al., 1998). In order to analyze the packing and flexibility of clathrin more precisely, we have used features of the program O (Jones et al., 1991), as described in Experimental Procedures, to build a model for clathrin triskelions in the lattice (Figures 3 and 4). Elements of secondary or tertiary structure cannot, of course, be discerned at this resolution, and we have defined the course of each leg as a set of points, connected sequentially along the uninterrupted stretches of density clearly seen in the map.

The barrel design for a clathrin lattice (Figure 1A) contains 36 triskelions or 108 individual legs (Crowther et al., 1976). The symmetry of the structure dictates that specifying three triskelions (nine legs) is sufficient to define the packing—all others are related to these three by symmetry operations (see positions marked with stars in Figure 1A). We therefore traced nine legs independently and reconstructed the complete barrel by applying the appropriate rotations. The model for each leg contains 125 points (numbered sequentially from vertex—the C terminus of the clathrin heavy chain —to tip—the N terminus). Because they are represented in O by α carbons, the points are 3.8 Å apart. The overall length of the trace is therefore approximately 475 Å, in good agreement with the contour of a rotary shadowed triskelion.

The fit of our model to the reconstruction is shown in Figure 3. The triskelion legs are represented as worm-like rods of constant, arbitrary diameter, smoothly connecting the 125 points used for the model (Figures 3C and 3D). The thickness of a leg, as defined by contour levels in the reconstruction, does not appear to vary significantly. The proximal legs lie outside the distal legs, and thus as one leg extends from the vertex of its triskelion, it gradually passes inward from the surface of the

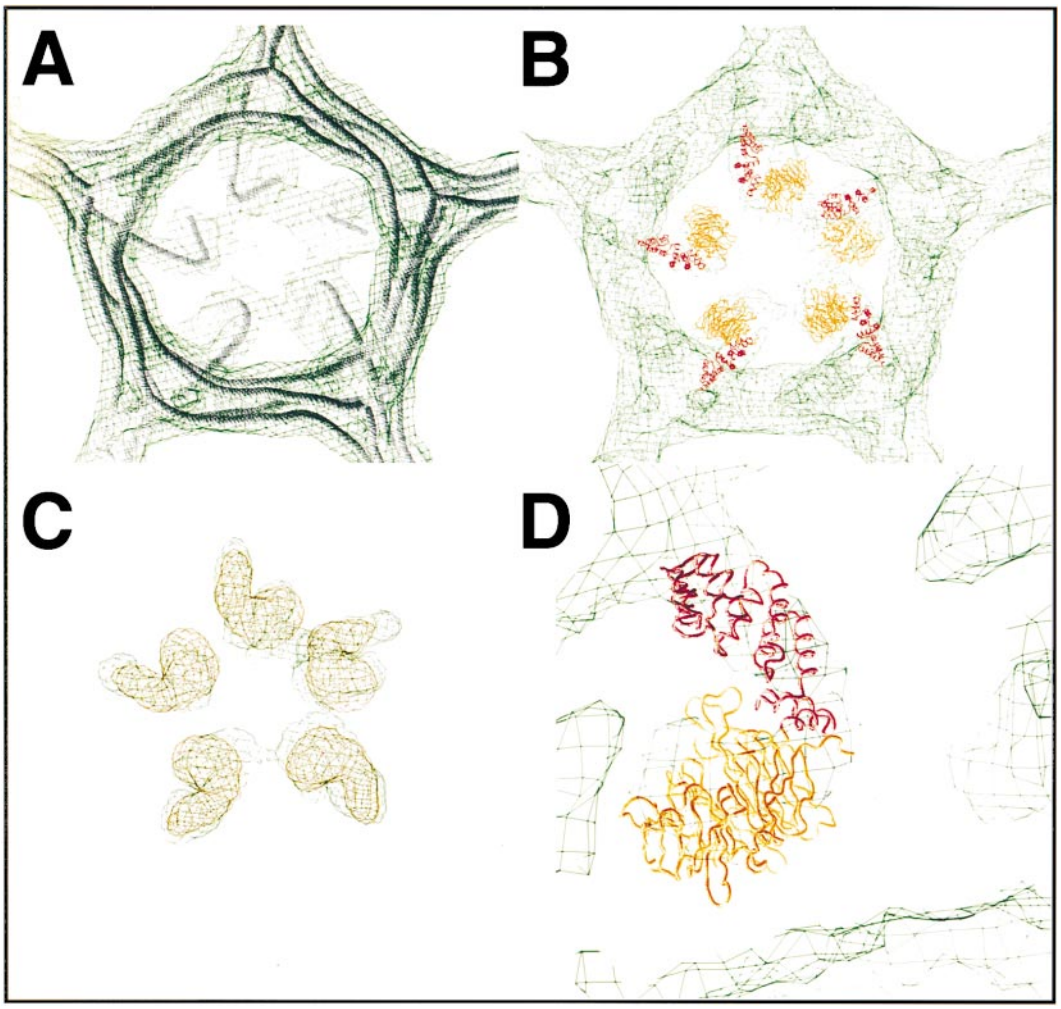

Figure 2. Fit of the Crystallographically Derived Model for the Terminal Domain and Linker to the CryoEM Image Reconstruction

(A) View through a pentagonal face, showing part of the triskelion model with its hook-like terminal domain.

(B) Similar view with a backbone representation of the high-resolution X-ray crystallographic model inserted into the same region of the map.

(C) Similar view with an electron density representation of the high-resolution X-ray model inserted into the hook-like terminal domains of the map.

(D) Close-up of a side view, showing the fit of one terminal domain. The feature at the lower margin of the figure represents the core of adaptor complexes present in the coat. In the molecular models, the β propeller is shown in yellow and the α zigzag in red.

barrel toward the interior (Figures 4A and 4B). Each edge of the coat contains two antiparallel proximal legs (red) and two antiparallel distal legs (green). Over the central part of an edge, the proximal and distal legs pack at relatively constant center-to-center distances: about 25 Å laterally between proximal (or distal) segments, and 20 Å radially between a proximal segment and the distal segment beneath it (Figure 4C). Although the resolution of the reconstruction does not allow the leg segments to be resolved clearly at all positions along an edge, the fit shown in Figure 3 is the only one that preserves continuity of the trace without invoking physically impossible crossovers. The knee, which is clearly resolved in the map (Figures 4A and 4B), has a relatively gradual bend. It skirts the vertex region of the barrel, so that the proximal and distal segments it connects border the same face (hexagon or pentagon) of the cage. This path is particularly clear in Figure 3D, where the leg on the right of the red triskelion in the center can easily be followed as it spans two edges of a hexagon and finally projects inward into the hook-like feature previously identified as the terminal domain. As described above, the fit of the crystallographically determined model of the terminal domain–linker to this density confirms the assignment.

The region around a vertex of the barrel contains a complex pattern of interactions (Smith et al., 1998). The reconstruction shows four clear layers in cross section (Figure 5). These correspond respectively to the hub of the triskelion centered on that barrel vertex, the knees of triskelions centered on the three neighboring vertices, and the distal legs and terminal domains from triskelions centered on second nearest–neighbor vertices. There appears to be a small globular element facing inward at the three-fold. Our model does not include any representation of this feature, which probably contains the

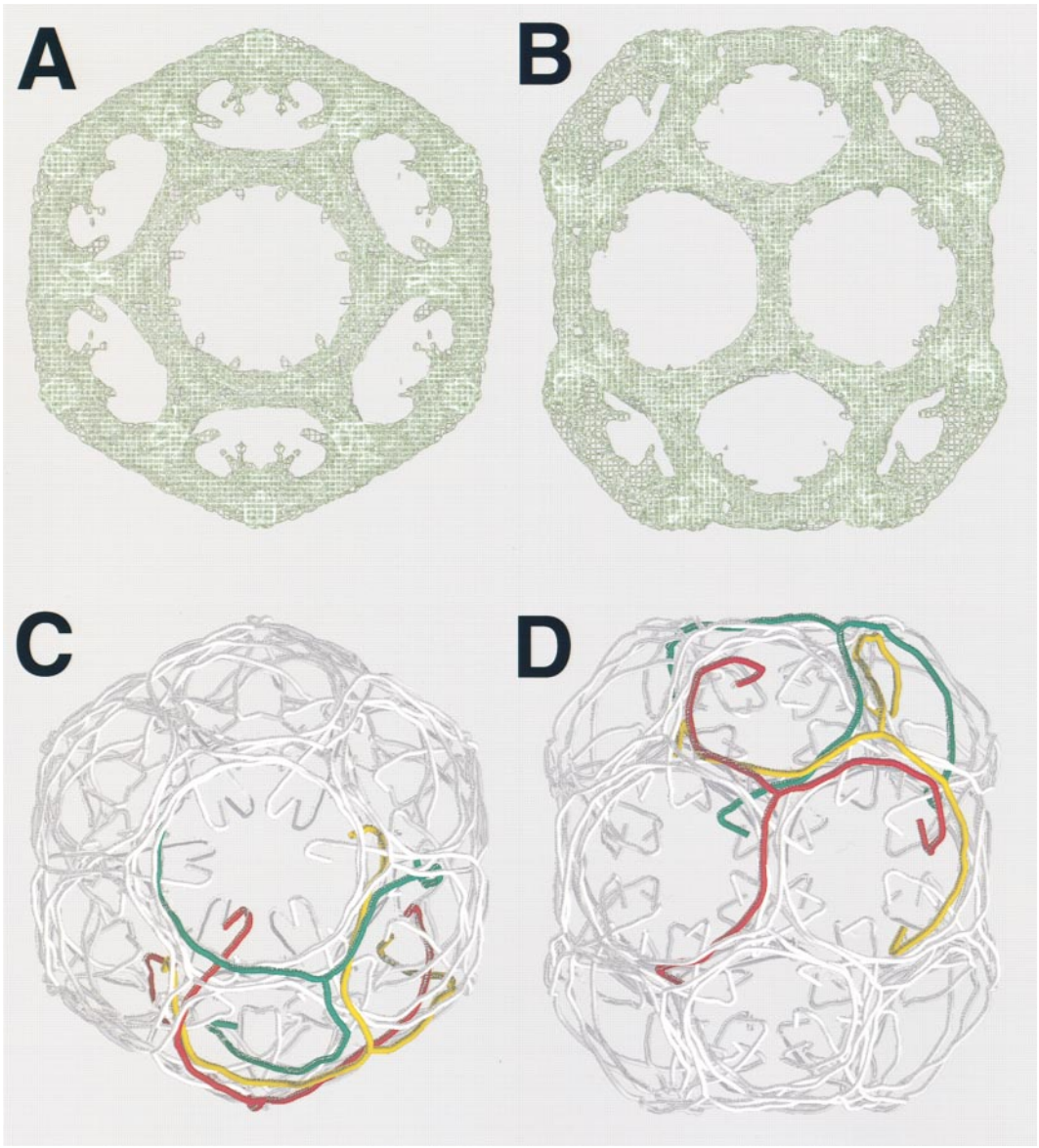

Figure 3. CryoEM Image Reconstruction of a Clathrin Barrel and Model for Triskelion Packing

(A and B) The EM reconstruction viewed along the six-fold (polar) and two-fold (equatorial) axes, respectively.

(C and D) Model of triskelions obtained as described in the text. Representatives of the three symmetry-independent triskelions are displayed in red, yellow, and green. The remaining triskelions, which were generated from these three by application of symmetry operations, are displayed in gray. The orientations of (C) and (D) correspond to the views in (A) and (B), respectively.

heavy chain C-terminal segments, known to be involved in trimerization (Kirchhausen and Harrison, 1984; Lemmon et al., 1991; Nathke et al., 1992; Pishvaee et al., 1997). Beneath the hub, distal legs and linkers (from triskelions centered two vertices away) form a three-way crossover, in which the center-to-center distance of the rods is about 20 Å. There appears to be a particularly tight interaction (arrows in Figure 5) between points 82–84 in the distal leg (about 315 Å from the hub) and points 93–95 in the linker (about 355 Å from the hub).

Triskelions

The model of a triskelion, excised from the coat, is shown in Figures 6A and 6B. Each leg bends relatively smoothly, with no sharp kinks, except at the boundary between linker and terminal domain (the hook). The clathrin light chains are known to be associated with the proximal segment of the heavy chain (Kirchhausen et al., 1983; Ungewickell, 1983; Kirchhausen and Toyoda, 1993). They are probably extended α helices where they attach to the heavy chain in defined regions, with disordered N- and C-terminal regions (Kirchhausen et al., 1987b; Scarmato and Kirchhausen, 1990; Nathke et al., 1992). They are therefore unlikely to contribute significantly to the apparent features of the reconstructed coat at this resolution. The most striking characteristic of the excised clathrin trimer is its pucker at the three-fold. The vertex lies approximately 240 Å above the plane

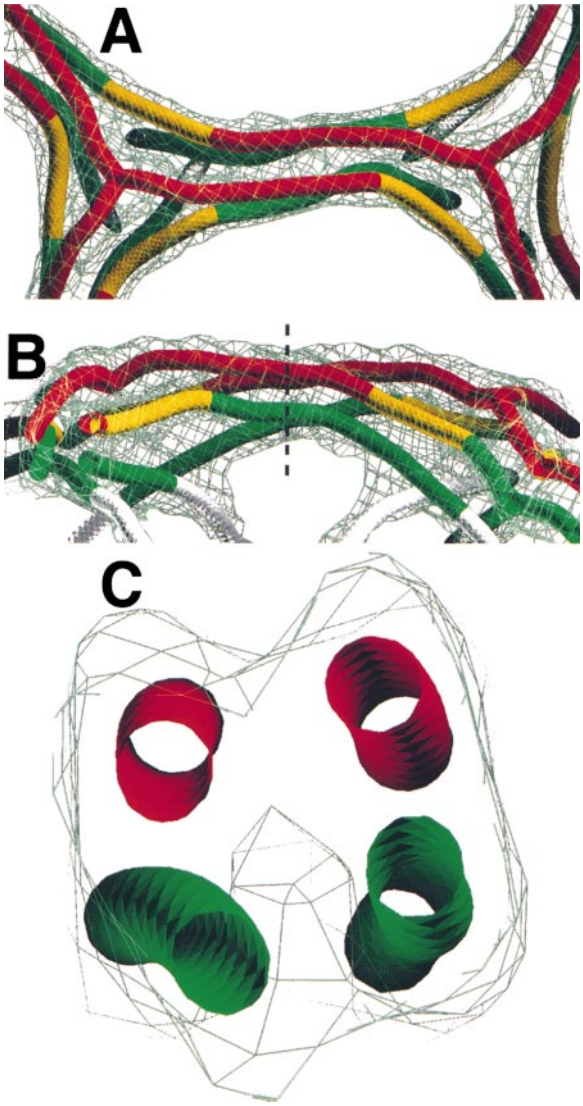

Figure 4. Fit of the Clathrin Triskelion Model to the EM Reconstruction

(A) View of an edge from outside the barrel (cytosol to membrane). The vertex-to-vertex distance is 185 Å.

(B) Side view of the same edge, rotated 90° relative to the orientation in (A). The upper part of the figure corresponds to the outside of the barrel.

(C) Slab-like cross section through the edge, centered at the position indicated by the dashed line in (B), showing the packing of proximal and distal legs. The color scheme is described in the caption to Figure 1.

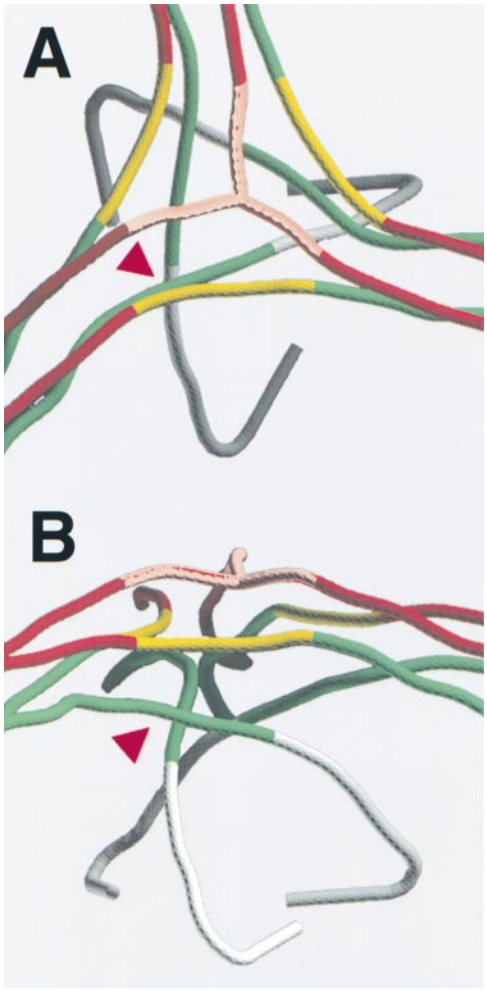

Figure 5. Appearance of the Model in the Region of a Barrel Vertex

The outermost structure is the vertex of a triskelion, which is centered on this vertex of the barrel. The contact-free zone of each leg near the triskelion vertex is in light red; the rest of the proximal leg is in darker red. Beneath the triskelion vertex are the knees (yellow) of three triskelions centered at neighboring barrel vertices. At still smaller radii are the distal legs (green) and linkers (gray) from triskelions centered two vertices away. The terminal domains (also gray) are at the innermost radii.

(A) View from outside the barrel.

(B) View at 90° from (A).

defined by the tips of the terminal domains. All three symmetry-independent trimers in the barrel have the same pucker (Figures 6C and 6D).

The fit of the terminal domain–linker fragment to the hook-like feature in the image reconstruction places the C terminus of the model (residue 490) close to point 93 in all nine symmetry-independent legs. As discussed in detail in the report of the high-resolution X-ray structure, the linear density of a clathrin leg is about three residues per angstrom. If we allow 75 residues for the trimerization domain not included in our model for a leg (Liu et al., 1995), the expected position of residue 490 would be point 87 in the model, about 1110 residues from the C terminus of the heavy chain, within reasonable agreement of the observed position. This agreement strengthens our confidence in the fit of the crystallographically derived model to the reconstructed density in the coat.

In the computed cryoEM reconstruction, the terminal domains are somewhat weaker than the rest of the triskelion. We interpret the lower density of the terminal domain features to be a consequence of the lack of constraints on the linker. Indeed, the point at which the strength of the computed reconstruction decreases is just where the linker emerges from passing under a distal leg—the last point of clearly defined intermolecular contact in the lattice (arrows in Figures 5A and 5B).

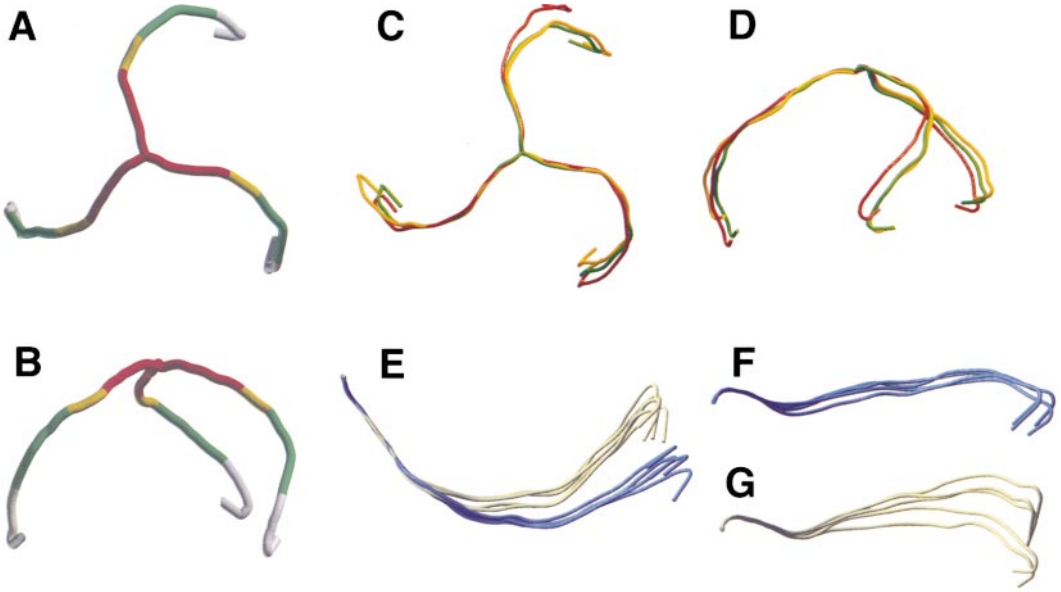

Figure 6. Three Dimensional View of a Single Triskelion and Superposition of Triskelions and Individual Legs from Different Positions in the Barrel

(A and B) A triskelion, colored as described in Figure 1A, has been excised from the model of a coat. The side view in (B) emphasizes the significant pucker of the clathrin molecule.

(C and D) Superpositions of the three unique triskelions in the barrel, colored as in Figure 3. The legs align well in the proximal region, but they diverge at the knee. Small divergences propagate into quite substantial changes in the relative positions of the terminal domains.

(E–G) Individual clathrin legs, aligned by superposition of their proximal segments. In (E), two groups of legs can be identified, characterized by different curvatures at the knee. The distal segment of legs depicted in blue face hexagons, while those in light yellow face pentagons. In (F) is shown a side view of the aligned "blue" legs, after rotation of 90° about a horizontal axis relative to the view in (E). In (G) is a side view of the "light yellow" legs, showing that there is a significant degree of divergence within this group, due to torsion of the rods.

The coats contributing to the reconstruction were assembled with AP-2 complexes. There are substoichiometric numbers of these complexes per barrel (roughly one adaptor complex per two triskelions) (Gallusser and Kirchhausen, 1993), and the symmetry of the AP-2 cluster near the center of the coat may not correspond to the symmetry of the clathrin lattice. Therefore, differently oriented interactions of the clathrin terminal domains with the hinge of AP β chains (the principal contact between clathrin and adaptor complexes) (Dell'Angelica et al., 1998; A. Contreras and T. K., unpublished data) could have pulled some of the terminal domains away from what would otherwise have been their equilibrium positions, decreasing the effective occupancy of the majority positions. Even when unconstrained by AP interactions, the linker may be somewhat more flexible than other parts of the leg.

The 108 terminal domains in the complete barrel form a remarkably tight intermediate layer facing the AP cluster. The "top" side of the β propeller faces toward the center of the coat, and the grooves along the perimeter of the propeller are radially aligned. Adaptor proteins are therefore likely either to contact the top surface of the terminal domain or to have a segment of polypeptide chain that extends outward along one of the seven grooves.

Triskelion Flexibility

Clathrin lattices have both pentagonal and hexagonal faces, and cages can also vary in radius (and hence in local curvature). Where in the clathrin molecule is the flexibility required by these properties of its assemblies? We have traced independently the nine legs of the three clathrin trimers that compose an "asymmetric unit" of the barrel, and we can therefore superpose the various legs in order to discern large scale differences in their conformations. Some aspects of this analysis are shown in Figures 6C–6G. From the superpositions in Figures 6C and 6D, it is clear that the vertices and proximal legs of the three symmetry-independent triskelions in the six-fold barrel are invariant in their conformations. Moreover, rotational superpositions show that the central portions of the trimers have essentially perfect three-fold axes. That is, when individual trimers in Figures 6A or 6B are rotated by 120° or 240° about axes through their vertices, the proximal legs coincide closely (data not shown). Thus, the trimerization domains at the center of the clathrin triskelion appear to have a fixed structure within this type of cage, and the capacity of clathrin to form pentagonal and hexagonal faces does not come from differences in interchain angle or pucker at the triskelion vertex. Rather, significant variation is restricted to the knees and distal legs. In the discussion section, we review evidence that the pucker of clathrin trimers in solution is very similar to the unique pucker we see in the barrel lattice. We also point out that in larger cages and flat arrays, the pucker is likely to decrease, and we suggest how this change might occur.

The flexibility within a leg is illustrated in Figures 6C–6E, which show superpositions based on the first 25 points (about 95 Å) of each leg. The chain conformations

cluster in two groups according to whether the leg borders a hexagonal or a pentagonal face (blue and light yellow, respectively, in Figures 6E–6G). Chains in the second group further cluster in subgroups that appear to have torsional differences (Figure 6G). At this resolution, it is not possible to assess whether the divergence in direction of the distal legs originates from one or more discrete hinges or whether the observed flexibility is more continuously distributed. Superposition of the distal legs (data not shown) does indicate a close agreement in this region of the molecule, suggesting that most of the variation seen in this structure is concentrated in the knee. The unusual length of the clathrin legs makes it easy for a small distortion at the knee to propagate into a major displacement of the terminal domain.

Discussion

Position and Orientation of the Terminal Domain

The 108 terminal domains project inward, and they do not appear to interact tightly with any other clathrin molecules. The first close contact that the linker makes with another clathrin heavy chain is at around points 82–84, corresponding to residue 537 from the C terminus (arrows in Figure 5). This fit to the reconstruction is consistent with the results of limited tryptic proteolysis of clathrin cages, which leads to preferential cleavage of the heavy chain at a position very close to residues K_{507} or R_{523} and to release of the terminal domain and linker without disruption of the lattice (Kirchhausen and Harrison, 1984; Kirchhausen et al., 1987a).

The nine symmetry-independent terminal domains all lie with the top surface of the β propeller facing the inner cluster of AP complexes. The propeller design has a set of grooves on its lateral surface, suitable for interaction with different adaptor proteins, and there is evidence that β-arrestin and arrestin-3, adaptors for the β adrenergic receptor, indeed contact one of these grooves through extended, C-terminal tails (Krupnick et al., 1997; Ter Haar et al., 1998; E. Ter Haar et al., personal communication). The observed orientation of the terminal domain would allow a projecting peptide, such as this C-terminal tail, to access any of the seven grooves around the perimeter of the propeller, while presenting the top surface for further contacts. The β subunit of heterotrimeric G proteins, also a seven-blade β propeller, interacts with the α subunit in this way: the top surface of the propeller contacts the Ras-like domain of Gα, while one of the grooves accepts a helical projection from the N terminus (Wall et al., 1995; Lambright et al., 1996). The likely orientation of the G protein β subunit with respect to the membrane is different from what we see in the clathrin cage, however.

Shape of a Triskelion and Flexibility along the Legs

The three symmetry-independent triskelions within the barrel have (to the accuracy of the present analysis) precise three-fold symmetry near their vertices and invariant pucker. Clathrin in free solution is likely to have a pucker quite similar to the one seen here, as shown previously by electron microscopy of triskelions in negative stain and also adsorbed onto mica and rotary shadowed after rapid freezing (Kirchhausen et al., 1986). The relatively symmetric images of trimers with a clockwise swirl (Crowther and Pearse, 1981; Kirchhausen and Harrison, 1981; Kirchhausen et al., 1986) had a narrow variation in distances between terminal domains (Kirchhausen et al., 1986), consistent with the interpretation that they came from puckered molecules such as the one in Figure 6B, adsorbed initially to the grids through their terminal domains (Kirchhausen et al., 1986). The average interterminal domain distance was about 450 Å, very similar to what we measure for the trimer models in the present work. This value of the span is closest to what might be expected (430 Å) from triskelions with all their legs in one configuration (the blue conformation in Figure 6). Such a trimer might be the "ground state" of clathrin, found in the absence of restraints from packing in a cage. By contrast with the clockwise images of mica-adsorbed clathrin, images having an anticlockwise swirl were often quite asymmetric, with widely varying distances (generally larger than in the clockwise images) between the tips of their legs (Kirchhausen et al., 1986). These pictures probably derived from molecules that landed "vertex first," with subsequent splaying outward of their legs against the mica surface.

It has been suggested that the clathrin light chains may govern the pucker of a triskelion and that this variation may in turn control the formation of hexagons and pentagons (Liu et al., 1995; Pishvaee et al., 1997; Pishvaee and Payne, 1998). Two earlier lines of evidence argue against this proposal. First, the overall pucker of free clathrin, revealed by electron microscopy as just described, is the same whether or not light chains are present (Kirchhausen et al., 1986). Second, light chains do not affect the curvature of the structures that are formed either in the presence or in the absence of adaptors (Winkler and Stanley, 1983; Lindner and Ungewickell, 1991; Ungewickell and Ungewickell, 1991). The data presented here are consistent with these observations: the differences among legs in cages occur beyond the proximal segments with which light chains are known to associate.

We suggest instead that the clathrin legs are stiff but not rigid structures that can flex in response to packing requirements. Within the barrel studied here, this flexion is concentrated in the knee. The α zigzag structure of the linker between terminal domain and distal leg has the characteristics necessary for a suitable compliant component (Ter Haar et al., 1998). The packing dimensions of the proximal and distal segments—about 20–25 Å (Figure 4C)—are consistent with the proposal that the α zigzag is the basic structure of the entire clathrin leg. The short helical hairpins in the clathrin linker α zigzag can rotate a bit with respect to each other and can also part slightly. Thus, the interactions between successive hairpins permit both twist and bend, and these mechanical properties of an α zigzag could impart to the knee its required flexibility.

Variable Curvature of Clathrin Lattices

Clathrin can form closed structures significantly larger than the barrel analyzed here, as well as extended hexagonal arrays. This variation probably involves a change in the pucker at the triskelion vertex to a value appropriate to the mean curvature of the shell rather than a

change in noncovalent contacts along the legs between triskelions. Altered contacts would require the proximal legs to cross each other at a different angle (looking tangentially, as in Figure 4B). The interactions extend over about 90 Å, and changing the crossing angle would involve major disruption and rearrangement. The structure of a cage in the vicinity of a vertex and the evident deformability of a leg near the knee suggest a simple way in which the effective pucker can also vary when required. Like the knee, the proximal leg near the vertex is free of contacts in the lattice (zone colored in lighter red in Figure 5). The relatively smooth bend of the knee ensures that this lack of contact will also be true in larger cages and flat arrays. If the molecular architecture of the proximal leg resembles that of the knee, then the contact-free zone near the vertex will be stiff but deformable (compare Figure 6), and relatively small forces will be able to open up the angle between the legs.

The equilibrium pucker of triskelions in solution (similar, as discussed above, to that of triskelions in the hexagonal barrel) will determine a preferred curvature or a range of curvatures for a lattice, as observed in the modest size range of cages produced by in vitro assembly of purified clathrin (Kirchhausen and Harrison, 1981; Pearse and Crowther, 1982). But, if contact-free segments of the leg are deformable, constraints such as assembly against a flat surface (e.g., where a cell adheres to a substrate) or assembly around a large diameter cargo (e.g., an adenovirus particle) can, according to our model, alter the curvature with relatively little free energy cost. Further adaptation can also occur at the knee. The actual trimer contacts at a clathrin vertex need not change, only the flexing of the contact-free heavy chain segment near the trimerization element. The required range of bending is no greater than what we observe among the different states of the knee in the barrel assembly itself. (Notice, for example, what sort of deformation near the vertex would be required to make the left-hand leg in Figure 6B project horizontally, and compare it with the range of angles of knee bends in Figure 6C or 6E). The deformability of the linker α zigzag, seen by comparing the three crystallographically distinct copies of the terminal domain–linker (Figure 7 in Ter Haar et al., 1998), would be adequate. The essential feature of this model is that the contents of a growing coat can help determine its curvature and prevent the abrupt termination of assembly that would occur if the lattice were to close off too tightly.

Clathrin Assembly and Disassembly on Membranes

The picture of a triskelion that emerges from our analysis is of a strongly puckered trimer with stiff legs and somewhat more flexibly linker terminal domains. How can such an assembly unit rapidly form a clathrin lattice, as observed both in vivo and in vitro? The packing illustrated in Figure 3 allows a triskelion to add readily to the growing edge of a lattice without having to insert between closely spaced legs from other molecules. Imagine, for example, rotating the red triskelion in Figure 3D slightly clockwise about its vertex. Its legs will smoothly disengage from their neighbors, and the entire trimer will be free to dissociate outward. The reverse of this process can ensure rapid addition at any stage in the formation of a coated vesicle lattice.

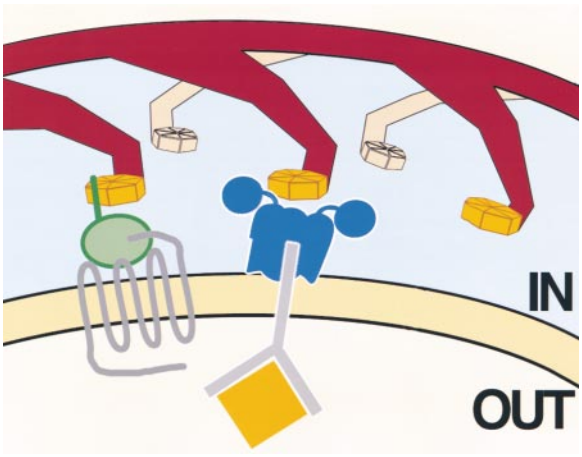

Figure 7. Schematic Representation of the Cross Section of an Invaginated Clathrin-Coated Membrane to Illustrate the Relative Disposition of Clathrin, Adaptors, and Cargo within the Clathrin Coat

The main part of the clathrin lattice is in red, with the distal end on the legs including the β propeller terminal domain and the α zigzag linker projecting toward the membrane. Receptors in the membrane contact adaptor proteins, which in turn interact with clathrin terminal domains. Members of the family of nonvisual arrestins (green) serve as adaptors for a number of seven transmembrane–helix proteins such as the β2 adrenergic receptor (left). The AP-1 and AP-2 complexes (blue) serve as adaptors for growth-factor receptors, transferrin receptors, and many others (center).

It has occasionally been suggested that hexagonal arrays of clathrin might rearrange locally into curved structures (Heuser, 1980). While this is not possible in the interior of the hexagonal lattice pinned down to a substrate, rapid disassembly and reassembly into curved structures at the edge of a flat array can cause it to appear to be feeding a growing coated pit. The ease of association and dissociation just described is compatible with these events. Indeed, the mechanism by which curvature can vary, proposed in the previous section, leads naturally to such a process. If the flat array represents a somewhat strained state of a triskelion, then wherever the cell surface lifts away from the substrate, disassembly from the hexagonal lattice and reassembly into a curved coat will be favored. Rapid equilibration between flat and curved structures is consistent with the known strength of clathrin association. Under physiological conditions, the stability of an assembled lattice is marginal, and coat formation in vitro requires interaction with adaptor complexes.

Adaptors and other factors specify in vivo that clathrin assembly will occur on a membrane and not free in the cytosol. In this work, we have used purified AP-2 adaptors, the plasma membrane–specific complex, to form coats. Similar coats can be formed using AP-1 from the *trans*-Golgi network. A flexible hinge segment from the adaptor β chain extends away from the body of the complex to interact with the clathrin terminal domain. The orientation of the terminal domain in the lattice, determined here, suggests that the hinge peptide could insert into one of the seven grooves on the lateral surface of the β propeller, probably with its amino end near the "top" face of the domain and the carboxyl end near the "bottom" face. The schematic drawing in Figure 7 illustrates how coat assembly relates spatially to the

adaptor complexes and to the receptors that they in turn recruit into coated pits. The nonvisual arrestins, which act as specific adaptors for the β adrenergic receptor and related molecules, have a flexible carboxyl-terminal peptide, which is known to interact in the groove between propeller blades 1 and 2. Its orientation, as it projects away from the membrane, is probably the same as that of the adaptor β chain hinge and therefore likewise consistent with the arrangement shown in Figure 7. Other molecules, such as amphiphysin, AP180, and epsin, may also interact with clathrin, but the nature of their interacting segments and their orientation with respect to clathrin have yet to be determined.

The prospects for obtaining higher resolution reconstructed images of clathrin assemblies by electron cryomicroscopy and the possibility of docking X-ray crystal structures into those maps promise in the near future substantially more detailed pictures of clathrin coats and coated vesicles.

Experimental Procedures

Analysis of the Path of a Clathrin Leg

To fit a set of points to the evident trace of a clathrin leg, we positioned a set of "pseudoatoms," using the program O (Jones et al., 1991). We created an initial skeleton by generating short linear arrays of points with an ad hoc computer program and displaying these arrays (about 10–20 pseudoatoms at an interatomic distance of 1.5 Å) with O. The short stretches were positioned in the map for the image reconstruction and edited until they produced a satisfactory fit. They were then assembled into a coordinate file. The initial skeleton consisted of nine chains, each composed of 330 pseudoatoms. The chains were edited on a chain-by-chain basis in order to improve their fit to the map. Differences in interatomic positions among chains that were introduced at this stage of model building were later removed when a new model was built with the "baton" command, using the initial model as a guide. Each new chain consisted of 125 pseudoatoms, at a fixed interatomic distance of 3.8 Å. Building and all subsequent analyses were carried out with O.

Fitting the Terminal Domain–Linker Structure to the CryoEM Reconstruction

It was first necessary to extract from the EM map the volume covering the terminal domain and linker. An initial manual placement of the coordinates at each of the nine symmetry-independent hook-like features in the map was made using O. A mask extending 20 Å around each atom in the PDB file was created using NCSMASK in the CCP4 suite (Collaborative Computational Project, 1994). The relevant regions of density were extracted from the map using masks and procedures created using the SPIDER image processing program (Frank et al., 1981, 1996), which was also used for subsequent operations. The PDB file containing the mask was converted to a volume of density with the same pixel sampling as the EM map, and both maps were filtered to exclude features above a resolution of 22 Å. A full six parameter search of orientation and position was conducted to find the best fit of the density derived from the crystal structure and the density derived from the EM map. The three position parameters were found by 3D cross-correlation of the maps. All relative orientations of the two maps were explored by applying rotations corresponding to a set of angles that cover all angular space with a sampling of better than 4°. Movements from the initial placement were within 15 Å and up to about 30°.

In seven of the nine cases, the orientation giving the best overall correlation coefficient conformed to known constraints derived from the biochemistry of the molecules. In the remaining two cases, the overall best fit corresponded to an orientation with N and C termini of the fragment reversed. Since this reversal was chemically unreasonable, the best correlation for a cone subtending 60° around the starting position was used to select the orientation of the fragment. The correlation coefficients between the X-ray and EM maps for the final positions of the terminal domains in the pentagonal face of the barrel were 0.68, 0.68, 0.73, 0.69, and 0.67. The correlation coefficient was 0.70 for the fit of the terminal domain in the hexagonal face on the six-fold symmetry axis of the barrel and 0.72 and 0.69 for the terminal domains in the equatorial hexagonal face on the two-fold symmetry axis. All approximate to 0.7, a value similar to what would be found for an outstanding molecular replacement solution in X-ray crystallography. In these experiments, the hand of the EM map chosen corresponds to the hand described for individual triskelions (Kirchhausen et al., 1986).

Acknowledgments

The work was supported in part by NIH grant GM36548 (T. K.). A. M. was an Armenise Fellow (Harvard Medical School Center for Structural Biology) and a Senior Postdoctoral Fellow of the American Cancer Society (Massachusetts Division). A. M. R. was supported on an EC TRANSNET grant, BI04-CT97–2119. S. C. H. is an Investigator in the Howard Hughes Medical Institute. We thank R. A. Crowther for helpful discussions. This paper is a contribution from the Harvard Medical School Center for Structural Biology, with support from the Harvard-Armenise Foundation for Advanced Medical Research.

Received March 8, 1999; revised April 28, 1999.

References

Ahle, S., Mann, A., Eichelsbacher, U., and Ungewickell, E. (1988). Structural relationships between clathrin assembly proteins from the Golgi and the plasma membrane. EMBO J. *7*, 919–929.

Benmerah, A., Lamaze, C., Begue, B., Schmid, S.L., Dautryvarsat, A., and Cerfbensussan, N. (1998). AP-2/Eps15 interaction is required for receptor-mediated endocytosis. J. Cell Biol. *140*, 1055–1062.

Chen, H., Fre, S., Slepnev, V.I., Capua, M.R., Takei, K., Butler, M.H., Difiore, P.P., and Decamilli, P. (1998). Epsin is an EH-domain-binding protein implicated in clathrin-mediated endocytosis. Nature *394*, 793–797.

Collaborative Computational Project, Number 4 (1994). The CCP4 suite: programs for protein crystallography. Acta Crystallogr. D *50*, 760–763.

Crowther, R.A., and Pearse, B.M. (1981). Assembly and packing of clathrin into coats. J. Cell Biol. *91*, 790–797.

Crowther, R.A., Finch, J.T., and Pearse, B.M. (1976). On the structure of coated vesicles. J. Mol. Biol. *103*, 785–798.

Cupers, P., Jadhav, A.P., and Kirchhausen, T. (1998). Assembly of clathrin coats disrupts the association between Eps15 and AP-2 adaptors. J. Biol. Chem. *273*, 1847–1850.

Dell'Angelica, E.C., Klumperman, J., Stoorvogel, W., and Bonifacino, J.S. (1998). Association of the AP-3 adaptor complex with clathrin. Science *280*, 431–434.

Frank, J., Shimkin, B., and Dowse, H. (1981). SPIDER—a modular software system for electron image processing. Ultramicroscopy *6*, 343–358.

Frank, J., Radermacher, M., Penczek, P., Zhu, J., Li, Y.H., Ladjadj, M., and Leith, A. (1996). Spider and web—processing and visualization of images in 3d electron microscopy and related fields. J. Struct. Biol. *116*, 190–199.

Gallusser, A., and Kirchhausen, T. (1993). The β1 and β2 subunits of the AP complexes are the clathrin coat assembly components. EMBO J. *12*, 5237–5244.

Goodman, O.B., Jr., Krupnick, J.G., Gurevich, V.V., Benovic, J.L., and Keen, J.H. (1997). Arrestin/clathrin interaction. Localization of the arrestin binding locus to the clathrin terminal domain. J. Biol. Chem. *272*, 15017–15022.

Heuser, J. (1980). Three-dimensional visualization of coated vesicle formation in fibroblasts. J. Cell Biol. *84*, 560–583.

Jackson, A.P., Seow, H.F., Holmes, N., Drickamer, K., and Parham, P. (1987). Clathrin light chains contain brain-specific insertion sequences and a region of homology with intermediate filaments. Nature *326*, 154–159.

Jones, T.A., Zou, J.-Y., and Cowan, S.W. (1991). Improved methods for building protein models in electron density maps and the location of errors in these models. Acta Crystallogr. A *47*, 110–119.

Kirchhausen, T., and Harrison, S.C. (1981). Protein organization in clathrin trimers. Cell *23*, 755–761.

Kirchhausen, T., and Harrison, S.C. (1984). Structural domains of clathrin heavy chains. J. Cell Biol. *99*, 1725–1734.

Kirchhausen, T., and Toyoda, T. (1993). Immunoelectron microscopic evidence for the extended conformation of light chains in clathrin trimers. J. Biol. Chem. *268*, 10268–10273.

Kirchhausen, T., Harrison, S.C., Parham, P., and Brodsky, F.M. (1983). Location and distribution of the light chains in clathrin trimers. Proc. Natl. Acad. Sci. USA *80*, 2481–2485.

Kirchhausen, T., Harrison, S.C., and Heuser, J. (1986). Configuration of clathrin trimers: evidence from electron microscopy. J. Ultrastruct. Mol. Struct. Res. *94*, 199–208.

Kirchhausen, T., Harrison, S.C., Chow, E.P., Mattaliano, R.J., Ramachandran, K.L., Smart, J., and Brosius, J. (1987a). Clathrin heavy chain: molecular cloning and complete primary structure. Proc. Natl. Acad. Sci. USA *84*, 8805–8809.

Kirchhausen, T., Scarmato, P., Harrison, S.C., Monroe, J.J., Chow, E.P., Mattaliano, R.J., Ramachandran, K.L., Smart, J.E., Ahn, A.H., and Brosius, J. (1987b). Clathrin light chains LCA and LCB are similar, polymorphic and share repeated heptad motifs. Science *236*, 320–324.

Kirchhausen, T., Bonifacino, J.S., and Riezman, H. (1997). Linking cargo to vesicle formation—receptor tail interactions with coat proteins. Curr. Opin. Cell Biol. *9*, 488–495.

Krupnick, J.G., Goodman, O.B., Jr., Keen, J.H., and Benovic, J.L. (1997). Arrestin/clathrin interaction. Localization of the clathrin binding domain of nonvisual arrestins to the carboxy terminus. J. Biol. Chem. *272*, 15011–15016.

Lambright, D.G., Sondek, J., Bohm, A., Skiba, N.P., Hamm, H.E., and Sigler, P.B. (1996). The 2.0 Å crystal structure of a heterotrimeric G protein. Nature *379*, 311–319.

Lemmon, S.K., Pellicena Palle, A., Conley, K., and Freund, C.L. (1991). Sequence of the clathrin heavy chain from Saccharomyces cerevisiae and requirement of the COOH terminus for clathrin function. J. Cell Biol. *112*, 65–80.

Lindner, R., and Ungewickell, E. (1991). Light-chain-independent binding of adaptors, AP180, and auxilin to clathrin. Biochemistry *30*, 9097–9101.

Liu, S.-H., Wong, M.L., Craik, C.S., and Brodsky, F.M. (1995). Regulation of clathrin assembly and trimerization defined using recombinant triskelion hubs. Cell *83*, 257–267.

Nathke, I.S., Heuser, J., Lupas, A., Stock, J., Turck, C.W., and Brodsky, F.M. (1992). Folding and trimerization of clathrin subunits at the triskelion hub. Cell *68*, 899–910.

Pearse, B.M., and Crowther, R.A. (1982). Packing of clathrin into coats. Cold Spring Harb. Symp. Quant. Biol. *46*, 703–706.

Pearse, B.M., and Robinson, M.S. (1984). Purification and properties of 100-kd proteins from coated vesicles and their reconstitution with clathrin. EMBO J. *3*, 1951–1957.

Pearse, B., and Robinson, M. (1990). Clathrin, adaptors, and sorting. Annu. Rev. Cell Biol. *6*, 151–171.

Perry, M.M., and Gilbert, A.B. (1979). Yolk transport in the ovarian follicle of the hen (Gallus domesticus): lipoprotein-like particles at the periphery of the oocyte in the rapid growth phase. J. Cell Sci. *39*, 257–272.

Pishvaee, B., and Payne, G.S. (1998). Clathrin coats—threads laid bare. Cell *95*, 443–446.

Pishvaee, B., Munn, A., and Payne, G.S. (1997). A novel structural model for regulation of clathrin function. EMBO J. *16*, 2227–2239.

Robinson, M.S. (1987). 100-kD coated vesicle proteins: molecular heterogeneity and intracellular distribution studied with monoclonal antibodies. J. Cell Biol. *104*, 887–895.

Robinson, M.S. (1997). Coats and vesicle budding. Trends Cell Biol. *7*, 99–102.

Scarmato, P., and Kirchhausen, T. (1990). Analysis of clathrin light chain-heavy chain interactions using truncated mutants of rat liver light chain LCB3. J. Biol. Chem. *265*, 3661–3668.

Schmid, S.L. (1997). Clathrin-coated vesicle formation and protein sorting: an integrated process. Annu. Rev. Biochem. *66*, 511–548.

Smith, C.J., Grigorieff, N., and Pearse, B.M. (1998). Clathrin coats at 21 Å resolution: a cellular assembly designed to recycle multiple membrane receptors. EMBO J. *17*, 4943–4953.

Sorger, P.K., Crowther, R.A., Finch, J.T., and Pearse, B.M. (1986). Clathrin cubes: an extreme variant of the normal cage. J. Cell Biol. *103*, 1213–1219.

Ter Haar, E., Musacchio, A., Harrison, S.C., and Kirchhausen, T. (1998). Atomic structure of clathrin—a beta propeller terminal domain joins an alpha zigzag linker. Cell *95*, 563–573.

Ungewickell, E. (1983). Biochemical and immunological studies on clathrin light chains and their binding sites on clathrin triskelions. EMBO J. *8*, 1401–1408.

Ungewickell, E., and Branton, D. (1981). Assembly units of clathrin coats. Nature *289*, 420–422.

Ungewickell, E., and Ungewickell, H. (1991). Bovine brain clathrin light chains impede heavy chain assembly in vitro. J. Biol. Chem. *266*, 12710–12714.

Vigers, G.P., Crowther, R.A., and Pearse, B.M. (1986a). Location of the 100 kd-50 kd accessory proteins in clathrin coats. EMBO J. *5*, 2079–2085.

Vigers, G.P., Crowther, R.A., and Pearse, B.M. (1986b). Three-dimensional structure of clathrin cages in ice. EMBO J. *5*, 529–534.

Wall, M.A., Coleman, D.E., Lee, E., Iniguez-Lluhi, J.A., Posner, B.A., Gilman, A.G., and Sprang, S.R. (1995). The structure of the G protein heterotrimer Gi alpha 1 beta 1 gamma 2. Cell *83*, 1047–1058.

Wigge, P., Vallis, Y., and McMahon, H.T. (1997). Inhibition of receptor-mediated endocytosis by the amphiphysin SH3 domain. Curr. Biol. *7*, 554–560.

Winkler, F.K., and Stanley, K.K. (1983). Clathrin heavy chain, light chain interactions. EMBO J. *2*, 1393–1400.

Ybe, J.A., Greene, B., Liu, S.H., Pley, U., Parham, P., and Brodsky, F.M. (1998). Clathrin self-assembly is regulated by three-light chain residues controlling the formation of critical salt bridges. EMBO J. *17*, 1297–1303.